$^{12}C+^{12}C$ elastic scattering potentials obtained by unifying phase-shift analysis with the modified Newton-Sabatier inverse method

Barnabás Apagyi,[1,2] Alexander Schmidt,[1] Werner Scheid,[1] and Helmut Voit[3]
[1]*Institut für Theoretische Physik der Justus-Liebig-Universität, D-35392 Giessen, Germany*
[2]*Quantum Theory Group, Institute of Physics, Technical University of Budapest, 1521 Budapest, Hungary*
[3]*Physikalisches Institut der Universität Erlangen-Nürnberg, Erlangen, Germany*
(Received 27 September 1993)

A procedure to connect a model-independent phase-shift analysis with the solution of the inverse quantum scattering problem has been developed and applied to experimental differential cross sections of $^{12}C+^{12}C$ elastic scattering in the energy range $E_{c.m.}$=8–12 MeV. The minimization of the error square function χ^2 is performed with respect to the spectral coefficients involved in the inverse procedure. Input quantities are measured differential cross sections; output results are complex potentials. The real part of the potentials, so obtained, is characterized by a pronounced minimum value of $-$(7–14) MeV at relative distances in the range 2.4–3 fm and by a Coulomb barrier of height 6–7 MeV in the outer region around $r \approx$ 8–9 fm. In addition a second minimum, very shallow or vanishing at some incident energies, is found to exist in the region 5–6 fm. The imaginary part of the potential exhibits positive maxima in those regions of radial distances where the real part has minimum values indicating a possible feedback effect of flux to the elastic channel. The overall energy dependence of the potentials shows a shape transition resulting in diminishing the outer potential minimum between $E_{c.m.}$ of 9 and 12 MeV. The inverted (real) potentials yield phase shifts of $\pi/2$ in those partial waves where resonances are known to exist. The procedure is tested by recalculating differential cross sections from the inverted energy-dependent potentials with the result that consistent agreement with the experimental input data is found.

PACS number(s): 03.65.Nk, 24.10.−i, 25.70.−z

I. INTRODUCTION

Traditionally the inverse scattering problem of elastic scattering in quantum mechanics [1] at fixed energy is solved in two steps. First the differential scattering cross section is analyzed by a minimization procedure [2] which leads to an appropriate set of phase shifts. Then these phase shifts are used in the inversion procedure to provide the optical potential [3]. A consistency test is performed in each case in order to control the accuracy of the potential by ensuring that its use in the Schrödinger equation reproduces the input phase shift data and, thereby, the underlying cross section.

In this paper we study the possibility of unifying these two separate steps of the inverse quantum scattering problem. As a basic method for the inversion procedure we use the modified Newton-Sabatier method [3,4]. The idea of the suggested new method is to perform the minimization search for the spectral coefficients $\{c_l\}$ involved in the Newton-Sabatier procedure, rather than for the phase shifts $\{\delta_l\}$ obtained by conventional analyses. The method proposed has the benefit of determining the potential for the case of collisions of identical particles with zero spin, where only even phase shifts δ_l ($l = 0, 2, 4, \ldots, l_{max}$) contribute to the cross section. In the usual inversion calculation one has to carry out an arbitrary interpolation procedure in order to obtain the odd phase shifts δ_l ($l = 1, 3, 5, \ldots, l_{max} - 1$) needed as additional input quantities for the usual method. In the present case the primary quantities to be varied are the entire set of the spectral coefficients $\{c_l\}$ ($l = 0, 1, 2, \ldots, l_{max}$) which determine uniquely the potentials via the modified Newton-Sabatier method [3,4]. As a by-product, the whole set of scattering phase shifts $\{\delta_l\}$ ($l = 0, 1, 2, \ldots, l_{max}$) is obtained within this new method. The set of odd phase shifts can be compared with the interpolated ones of the conventional method.

For the practical application of our method we have chosen elastic scattering data of ^{12}C on ^{12}C in a range of $E_{c.m.}$ from 8 to 12 MeV out of a larger set of measured angular distributions. They belong to a set of 320 angular distributions of the $^{12}C+^{12}C$ elastic scattering measured at the Erlangen tandem accelerator between $E_{c.m.}$=6 and 14 MeV in energy steps of 25 keV. Of this set of data, we inverted the differential cross sections at $E_{c.m.}$=9.50 and 11.38 MeV previously [5], with the usual two-step procedure, applying a phase-shift analysis and the modified Newton-Sabatier method separately. Some of these data have been used already in the publications given in Ref. [6] to deduce the total reaction cross section and to determine $^{12}C+^{12}C$ resonances and their widths.

In Sec. II the model independent phase-shift analysis and the unified method of the inverse scattering problem are described together with the traditional procedure. In Sec. III A, the results of an exploratory calculation at a selected energy of $E_{c.m.}$=7.988 MeV are given. The results obtained for the inverted elastic scattering potential of the $^{12}C+^{12}C$ system are presented and discussed in Sec. III B for incident energies between $E_{c.m.}$=8 and 12 MeV. The summary and comments are given in Sec. IV.

II. METHODS

A. Phase-shift analysis

The differential cross section of the elastic scattering of two identical particles with zero spin is given by [7]

$$\frac{d\sigma(\theta)}{d\Omega} = |f(\theta) + f(\pi - \theta)|^2. \quad (1)$$

The scattering amplitude f can be written as

$$f(\theta) = f_C(\theta) + f_n(\theta), \quad (2)$$

where f_C is the Coulomb-scattering amplitude

$$f_c(\theta) = -\frac{\eta}{2k\sin^2(\theta/2)} \exp\left\{2i\sigma_0 - 2i\eta \ln\left(\sin\frac{\theta}{2}\right)\right\}, \quad (3)$$

and f_n the nuclear scattering amplitude

$$f_n(\theta) = \frac{1}{2ik}\sum_l (2l+1)e^{2i\sigma_l}(S_l - 1)P_l(\cos\theta). \quad (4)$$

In the equations above the Sommerfeld parameter η is given by $\eta = Z_P Z_T e^2/\hbar v$ where v is the relative velocity between projectile and target with charges Z_P and Z_T, respectively; the wave number k is expressed by $k = (2\mu E_{\text{c.m.}})^{1/2}/\hbar$ where the center-of-mass scattering energy is denoted by $E_{\text{c.m.}}$ and the reduced mass by $\mu = m_P m_T/(m_P + m_T)$. The Coulomb scattering phase shifts are defined by $\sigma_l = \arg\Gamma(l+1+i\eta)$. The S-matrix elements S_l can be expressed by the nuclear phase shifts δ_l as

$$S_l = e^{2i\delta_l}. \quad (5)$$

As the nuclear phase shifts are complex numbers,

$$\delta_l = \delta_l^R + i\delta_l^I, \quad (6a)$$

the S_l matrix elements can be written in the form

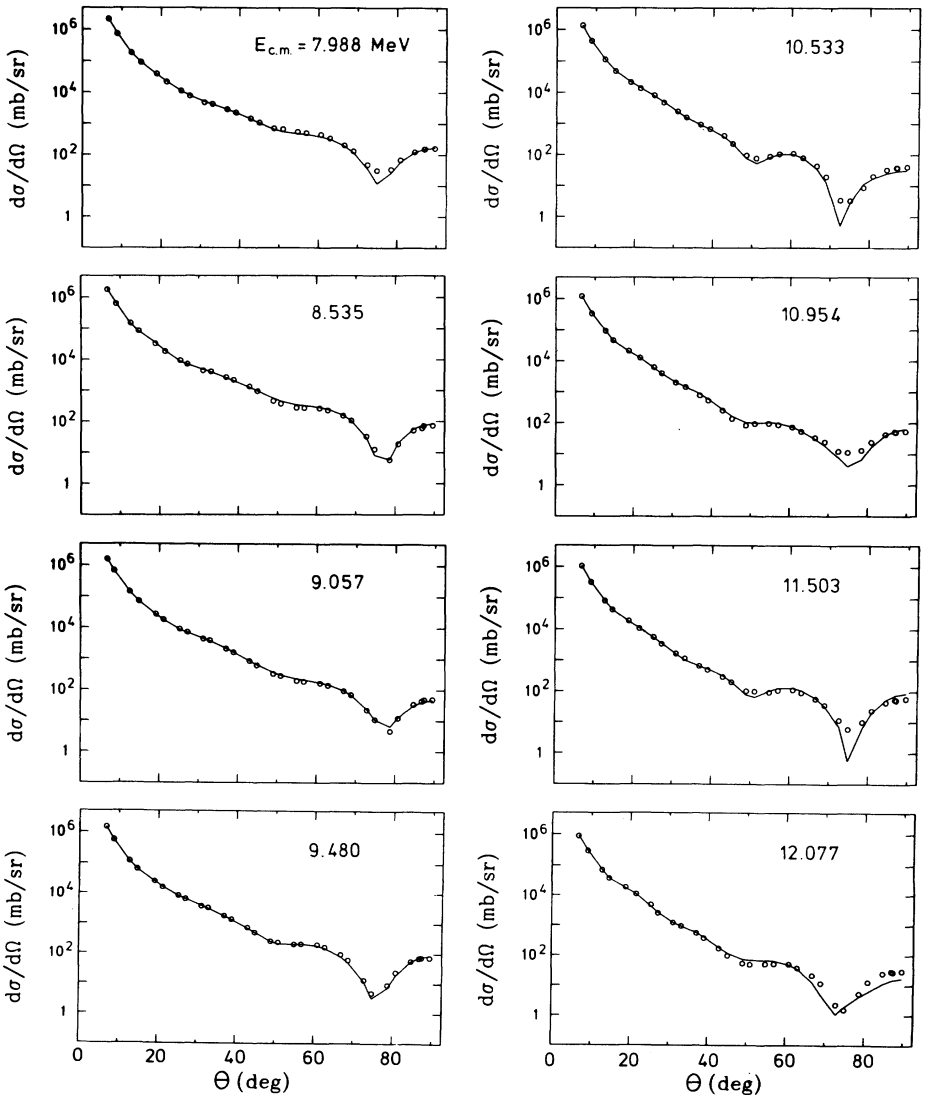

FIG. 1. Differential cross sections (o o o) measured by Voit and co-workers at the c.m. scattering energies indicated. Reproduction (——) of the experimental data by the inverted potentials shown in Fig. 5.

$$S_l = \eta_l e^{2i\delta_l^R} \tag{6b}$$

with the absorption coefficients defined by

$$\eta_l = e^{-2\delta_l^I}. \tag{6c}$$

The method of model independent phase-shift analysis consists of minimizing the error square function for N data points,

$$\chi_S^2 = \frac{1}{N}\sum_{i=1}^{N}\left(\frac{d\sigma(\theta_i)/d\Omega|_{\rm exp} - d\sigma(\theta_i)/d\Omega|_{\rm cal}}{\Delta d\sigma(\theta_i)/d\Omega}\right)^2, \tag{7a}$$

with respect to the sets $\{S_l\}$ or $\{\delta_l\}$ $(l = 0, 2, 4, \ldots, l_{\max})$ contained in the expression $d\sigma(\theta_i)/d\Omega|_{\rm cal}$. The quantities $d\sigma(\theta_i)/d\Omega|_{\rm exp}$ and $\Delta d\sigma(\theta_i)/d\Omega$ denote, respectively, the experimental differential cross sections and the absolute errors. These data are shown by circles in Fig. 1 for the energies considered in this paper.

The error square expression (7a) is constructed in such a way that terms with large relative errors are suppressed. Therefore, sometimes it proved useful to work with a modified error square function giving large weights to the small values of the differential cross sections which are the most interesting ones from the standpoint of quasimolecular resonances. This modified error square function is defined as

$$\chi'^2_S = \frac{1}{N}\sum_{i=1}^{N}\left(\frac{d\sigma(\theta_i)/d\Omega|_{\rm exp} - d\sigma(\theta_i)/d\Omega|_{\rm cal}}{d\sigma(\theta_i)/d\Omega|_{\rm exp}}\right)^2. \tag{7b}$$

To distinguish between the conventional phase-shift analysis (carried out by minimizing χ_S^2 or χ'^2_S with respect to the phase shifts) and the one used in this paper, we introduce the error squares χ_c^2 and χ'^2_c. These are defined by the expressions of Eqs. (7a) and (7b) with $d\sigma(\theta_i)/d\Omega|_{\rm cal}$ evaluated in our unified inverse scattering procedure using a set of spectral coefficients $\{c_l\}$ $(l = 0, 1, \ldots, l_{\max})$, as indicated by the suffix c. This procedure will be explained later.

To measure the quality of the inverted potentials we calculate a square error function χ_V^2, defined by Eq. (7a) save that $d\sigma(\theta_i)/d\Omega|_{\rm cal}$ is replaced by the differential cross sections $d\sigma(\theta_i)/d\Omega|_{\rm pot}$ calculated with the inverted potential V.

Since the minimization procedures are very time consuming and might depend sensitively on the starting point of the calculation, use has been made [8] of two searching methods. The first is the controlled random search (CRS) procedure [9] which determines the global minimum of a given function of n variables. The other is the pattern search (PS) method [10] which searches for the relative minima of a given function of n variables. This latter method depends very sensitively on the initial starting point of the search.

B. The modified Newton-Sabatier method

As shown by Newton [1], the reduced (dimensionless) potential of a scattering process with spherical symmetry can be calculated from the equation

$$U(\rho) = U_0(\rho) - \frac{2}{\rho}\frac{d}{d\rho}\sum_{l=0}^{\infty} c_l^U \varphi_l^{U_0}(\rho)\varphi_l^U(\rho)/\rho, \tag{8}$$

where the functions $\varphi_l^{U_0}(\rho)$ are the regular solutions of the radial Schrödinger equation for a given reference potential $U_0(\rho)$. The spectral coefficients c_l^U satisfy a system of coupled equations for the functions, $\varphi_l^U(\rho)$, that are the solutions of the radial Schrödinger equation with the potential U. Those solutions are given by

$$\varphi_l^U(\rho) = \varphi_l^{U_0}(\rho) - \sum_{l'=0}^{\infty} c_{l'}^U L_{ll'}(\rho)\varphi_{l'}^U(\rho) \tag{9}$$

in which the matrix is specified by

$$L_{ll'}(\rho) = \int_0^\rho \varphi_l^{U_0}(\rho')\varphi_{l'}^{U_0}(\rho')d\rho'/\rho'^2. \tag{10}$$

The functions $\varphi_l^U(\rho)$ obey the asymptotic condition

$$\varphi_l^U(\rho \to \infty) = A_l^U \sin(\rho - l\pi/2 + \delta_l + \sigma_l - \eta \ln 2\rho), \tag{11}$$

where A_l^U are normalization constants set by the inversion procedure and $\delta_l + \sigma_l$ are the total phase shifts due to the potential $U(\rho)$. The logarithmic term in the argument is because of the Coulomb interaction, which we include for nuclear heavy ion collisions. In the Eqs. (8)–(11), ρ and U are dimensionless quantities from which the radius r and the physical potential $V(r)$ can be obtained by setting $r = \rho/k$ and $V(r) = E_{\rm c.m.}U(\rho)$.

The modification of the method defined by Eqs. (8)–(11) is based on the fact that in heavy ion collisions the potential is known from a finite radius r_0 up to infinity. In such cases it is convenient to set

$$U(\rho) = U_0(\rho) \quad \text{for } \rho \geq \rho_0 = kr_0 \tag{12}$$

and to replace the infinite sum in Eq. (9) by a finite one running up to $l_{\max}$ that has a correspondence with the distance ρ_0. As proven by Münchow and Scheid [3], the solution for $U(\rho)$ becomes then unique in the class of potentials (8) defined by the Newton-Sabatier method. In this modified method the solution functions $\varphi_l^U(\rho)$ are known for $\rho \geq \rho_0$ and can be written as

$$\varphi_l^U(\rho \geq \rho_0) = A_l^U \rho[\cos\delta_l F_l(\rho) + \sin\delta_l G_l(\rho)], \tag{13}$$

where F_l and G_l denote the regular and irregular Coulomb functions [11], respectively.

For the reference potential, a natural choice is $U_0(\rho) = 2\eta/\rho_0$ for $\rho \leq \rho_0$ and $U_0(\rho) = 2\eta/\rho$ for $\rho \geq \rho_0$. But it is more convenient [4,12] to require $U_0(\rho) = 2\eta/\rho_0$ =const on the whole axis $0 \leq \rho \leq \infty$ and to shift the scattering energy $E_{\rm c.m.}$ to $E^B = E_{\rm c.m.} - 2\eta/\rho_0$. Then we have to transform the input phase shifts δ_l to δ_l^B by equating the logarithmic derivatives

$$\frac{d}{dr}\ln\varphi_l^B(r)\Big|_{r=r_0} = \frac{d}{dr}\ln\varphi_l^U(r)\Big|_{r=r_0}, \tag{14}$$

where the transformed functions

$$\varphi_l^B(\rho \geq \rho_0) = A_l^B k_B r[\cos\delta_l^B\, j_l(k_B r) - \sin\delta_l^B\, n_l(k_B r)] \quad (15)$$

correspond to the solution functions of the shifted problem in the outer region, and $k_B = (2\mu E^B)^{1/2}/\hbar$.

Then the set of equations of the inverse quantum scattering problem used in the modified Newton-Sabatier method reads ($\tilde{\rho} = k_B r$),

$$U^B(\tilde{\rho}) = -\frac{2}{\tilde{\rho}}\frac{d}{d\tilde{\rho}}\sum_{l=0}^{l_{\max}} c_l^B \varphi_l^0(\tilde{\rho})\varphi_l^B(\tilde{\rho})/\tilde{\rho}, \quad (16)$$

$$\varphi_l^B(\tilde{\rho}) = \varphi_l^0(\tilde{\rho}) - \sum_{l'=0}^{l_{\max}} c_{l'}^B L_{ll'}^B(\tilde{\rho})\varphi_{l'}^B(\tilde{\rho}), \quad (17)$$

and

$$L_{ll'}^B(\tilde{\rho}) = \int_0^{\tilde{\rho}} \varphi_l^0(\rho)\varphi_{l'}^0(\rho)d\rho/\rho^2, \quad (18)$$

with $\varphi_l^0(\tilde{\rho}) = \tilde{\rho} j_l(\tilde{\rho})$ being the regular solutions belonging to the (shifted) reference potential $U_0^B \equiv 0$.

C. The unified procedure

One starts by rewriting Eq. (17) in the form

$$\sum_{l'=0}^{l_{\max}} M_{ll'}^B(\tilde{\rho})\varphi_{l'}^B(\tilde{\rho}) = \varphi_l^0(\tilde{\rho}), \quad l = 0,1,\ldots,l_{\max} \quad (19)$$

by introducing the matrix

$$M_{ll'}^B(\tilde{\rho}) = \delta_{ll'} + L_{ll'}^B(\tilde{\rho})c_{l'}^B. \quad (20)$$

By giving a set of coefficients $\{c_l^B\}$ ($l = 0,1,2,\ldots,l_{\max}$), the matrix $\mathbf{M}^B$ is specified and one can calculate the unknown functions $\varphi_l^B(\tilde{\rho}_i)$ from Eq. (19) at any point of $\tilde{\rho}_i = k_B r_i$. If the calculation is performed at $N \geq 2$ points of $\tilde{\rho} > \tilde{\rho}_0$, the obtained values of $\varphi_l^B(\tilde{\rho}_i; c_0^B, c_1^B, \ldots, c_{l_{\max}}^B)$ can be applied to determine the phase shifts δ_l^B ($l = 0,1,2,\ldots,l_{\max}$) by using Eq. (15). One may then transform δ_l^B to δ_l [by virtue of Eq. (14)] and calculate the cross sections $d\sigma(\theta_i)/d\Omega|_{\rm cal}$ [via Eq. (1)] which should be used to minimize either χ_c^2 or χ'^2_c introduced in Sec. II A in connection with Eqs. (7).

There are two methods one may use to calculate the phase shifts δ_l^B with the modified Newton-Sabatier equations given in Eq. (19). The first possibility, identified hereafter as "method 1" (M1), is to solve ($\tilde{\rho}_i \geq \tilde{\rho}_0$)

$$\tilde{\rho}_i j_l(\tilde{\rho}_i)x - \tilde{\rho}_i n_l(\tilde{\rho}_i)y = \varphi_l^B(\tilde{\rho}_i; c_0^B, c_1^B, \ldots, c_{l_{\max}}^B),$$

$$i = 1,\ldots,N. \quad (21a)$$

Equation (21a) represents N equations for the two unknowns (l is fixed)

$$x = A_l^B\cos\delta_l^B, \quad y = A_l^B\sin\delta_l^B \quad (21b)$$

in each partial wave $l = 0,1,\ldots,l_{\max}$. Then the phase shifts can be determined as $\delta_l^B = \arctan(y/x) \bmod n\pi$. The other possibility, which we designate as "method 2" (M2), consists of solving the overdetermined system of equations ($\tilde{\rho}_i \geq \tilde{\rho}_0$)

$$\sum_{l'=0,1,\ldots}^{l_{\max}} M_{ll'}^B(\tilde{\rho}_i)\tilde{\rho}_i j_{l'}(\tilde{\rho}_i)x_{l'} - \sum_{l'=0,1,\ldots}^{l_{\max}} M_{ll'}^B(\tilde{\rho}_i)\tilde{\rho}_i n_{l'}(\tilde{\rho}_i)y_{l'} = \varphi_l^0(\tilde{\rho}_i),$$

$$i = 1,\ldots,N, \quad l = 0,1,\ldots,l_{\max} \quad (22a)$$

for the $2(l_{\max}+1)$ unknowns

$$x_l = A_l^B\cos\delta_l^B, \quad y_l = A_l^B\sin\delta_l^B,$$

$$l = 0,1,\ldots,l_{\max}, \quad (22b)$$

and of calculating the phase shifts from $\delta_l^B = \arctan(y_l/x_l) \bmod(n\pi)$. The two methods coincide for $N = 2$.

We applied the optimization procedures CRS [9] and PS [10], to determine an optimum set of the spectral coefficients $\{c_l^B\}$. In the case of the PS procedure it is useful to start with a set of $\{c_l^B\}$ obtained by the conventional inverse scattering calculation with interpolated values for the odd phase shifts. That set of values subsequently is optimized by the search. In the case of the CRS optimization no convergence of the search has been found within a reasonable interval of computational time (several hours on an IBM 3090-60J machine), mainly because the error square functions defined by Eqs. (7) for $^{12}C+^{12}C$ scattering are not sensitive to the odd l-value phase shifts and thence upon their effect in the spectral coefficients $\{c_l^B\}$ ($l = 0,1,\ldots,l_{\max}$). A way out of this dilemma would be to introduce restrictions on the values of $\delta_{l=\rm odd}^B$, but we do not intend to explore this possibility in the present work. Therefore, we used the PS procedure in the applications of the unified method that are described herein.

To make a distinction between methods M1 and M2 which are based on the minimization of χ_c^2 and those based on χ'^2_c, respectively, we designate results found using these latter methods by a prime, i.e., as M'1 and M'2.

III. RESULTS

A. The optical potential of the scattering system $^{12}C+^{12}C$ at $E_{\rm c.m.}$=7.998 MeV calculated by using different inverse scattering methods

First we made a conventional calculation at one selected energy ($E_{\rm c.m.}$=7.988 MeV). The minimization of the error square χ_S^2 yielded a set of phase shifts $\{\delta_l\}$

($l = 0, 2, \ldots, l_{\max}$) which were then used in the inverse scattering calculation to obtain potentials. This test calculation served also as a starting point for the unified method in which an initial guess of the spectral coefficients $\{c_l\}$ ($l = 0, 1, \ldots, l_{\max}$) is required. We have applied both CRS and PS methods to the phase-shift analysis and obtained different values of $\chi^2_S = 6.56$ and 6.79 with those methods, respectively. The initial S matrix for the PS procedure was taken to be $\mathrm{Re}S_l = 1$ and $\mathrm{Im}S_l = 0$ for the even values of l. With this choice for the initial point of the PS procedure we found agreement with the CRS results at the considered energies $E_{\mathrm{c.m.}} = 8.535$, 10.954, and 11.503 MeV. In order that the results of the phase-shift analysis correspond to the global minimum point of the $2l_{\max}+2$ dimensional space of the parameters $\mathrm{Re}S_l$ and $\mathrm{Im}S_l$ ($l = 0, 2, \ldots, l_{\max}$), we used the CRS method whenever a conventional phase-shift analysis of the scattering data was made.

The procedure consisting of the search for the phase shifts with even l's and of the subsequent conventional inversion calculation (with interpolated phase shifts for odd l's) will be designated "method C1" to distinguish it from the unified methods investigated in this work.

The matrix elements S_l ($l = 0, 2, \ldots, l_{\max}$) determined by the CRS phase-shift analysis of the ^{12}C+^{12}C scattering data at $E_{\mathrm{c.m.}}$=7.988 MeV are given in columns 2 and 3 of Table I. In columns 4 and 5 of Table I the real part of the phase shifts δ_l^R and the absorption coefficients η_l are listed together with the interpolated values for the odd partial waves as are needed in the conventional inversion calculation. The condition of getting a smooth potential shape has made it necessary to set $\mathrm{Re}\delta_7 = \delta_7 = -1.5$ and $\eta_7 = 0.2$. They are not interpolated values. A similar setting was found previously when we inverted scattering data at $E_{\mathrm{c.m.}} = 9.50$ MeV [5]. Note that the proximity of the scattering energy $E_{\mathrm{c.m.}} = 7.988$ MeV to the energy region of 7–8 MeV of the observed 4^+ shape resonances of the ^{12}C+^{12}C system [13] would also allow us to tune the phase shift and absorption coefficient belonging to the $l = 5$ partial wave. However, the variation of δ_5^R, and η_5 instead of δ_7^R, and η_7 did not result in a smooth potential shape upon inversion.

Figure 2 exhibits the inverted potentials together with the recalculated differential cross sections. There is a deviation from the measured (input) data at angles between 70° and 90° and, therefore, the potential cannot be considered to be consistent with the input data. This is also reflected by the large value of $\chi^2_V = 609.8$. A closer inspection of the data shows that the reproduction is unsatisfactory in those angular regions where the relative errors of the data are the largest. This fact enables us to introduce the modified error expression χ'^2_S as given by Eq. (7b), with which the data with larger relative errors are allowed to contribute more significantly. Although the S-matrix elements obtained by minimizing χ'^2_S are quite different from those found before (compare columns 6 and 7 of Table I with columns 2 and 3 of Table I), the potential shown in Fig. 2(c) that results from the conventional inversion calculation differs from the preceding one [see Fig. 2(a)] only in the internal region, a region which does not contribute too much in cross section calculations. However, the difference is sufficient for a better reproduction of the experimental cross section data [see Fig. 2(d)]. That is confirmed also by the corresponding smaller error square value of χ^2_V=60.8. A further advantage is that only δ_7^R, but not η_7, had to be varied to get a smooth potential shape (see columns 8 and 9 of Table I). We call this type of the conventional inversion calculation as "method C′1." The technical parameters have been kept fixed at $r_0 = 10$ fm, $\tilde{\rho}_i$=11.5, 12.5, 13.5, and $l_{\max}$=12 for both methods C1 and C′1.

Figures 3(a), 3(c), and 4(a), 4(c), show the potentials obtained by the unified procedures M1, M′1, and M2, M′2, respectively. The consistency of these calculations is exhibited in Figs. 3(b), 3(d), and 4(b), 4(d) which are characterized by the corresponding error square val-

TABLE I. Real and imaginary parts of the matrix elements S_l obtained by the conventional phase-shift analyses $C1$ and $C'1$ of the ^{12}C+^{12}C scattering data [6] at $E_{\mathrm{c.m.}} = 7.998$ MeV and based on the error square expressions χ^2_S and χ'^2_S given by Eqs. (7). The real phase shifts, δ_l^R, and absorption coefficients, η_l, are listed as well, together with the interpolated values for the odd partial waves. δ_7^R has been treated as a free parameter in order to obtain a smooth potential. In the case of method C1, η_7 has to be varied also. The potentials and cross sections corresponding to this table are shown in Fig. 2.

l	$\mathrm{Re}S_l$[a]	$\mathrm{Im}S_l$[a]	δ_l^{R}[a]	η_l[a]	$\mathrm{Re}S_l$[b]	$\mathrm{Im}S_l$[b]	δ_l^{R}[b]	η_l[b]
0	−0.5060	−0.8626	8.3741	1.0000	0.2897	−0.3257	9.0029	0.4359
1			6.9065	0.5809			7.2594	0.5454
2	−0.0190	−0.1607	5.4389	0.1618	0.0237	−0.6545	5.5159	0.6549
3			4.4583	0.4928			4.2545	0.4480
4	0.6446	0.5130	3.4777	0.8239	0.2305	−0.0706	2.9931	0.2410
5			1.7783	0.9053			1.3881	0.4503
6	0.9745	0.1550	0.0789	0.9868	0.5984	−0.2771	−0.2168	0.6595
7			−1.5000	0.2000			−1.5000	0.7348
8	0.8205	0.2877	0.1686	0.8695	0.7825	−0.2094	−0.1308	0.8100
9			0.1021	0.8634			−0.1143	0.9050
10	0.8551	0.0609	0.0356	0.8573	0.9809	−0.1944	−0.0978	1.0000
11			0.0061	0.8891			−0.0620	1.0000
12	0.9200	−0.0431	−0.0234	0.9210	0.9986	−0.0522	−0.0261	1.0000

[a]Method C1: minimization of χ^2_S (with the result $\chi^2_S = 6.54$; the corresponding inverted potential gives $\chi^2_V = 609.8$).
[b]Method C′1: minimization of χ'^2_S (with the result χ'^2_S =0.00135; the corresponding inverted potential gives $\chi^2_V = 60.8$).

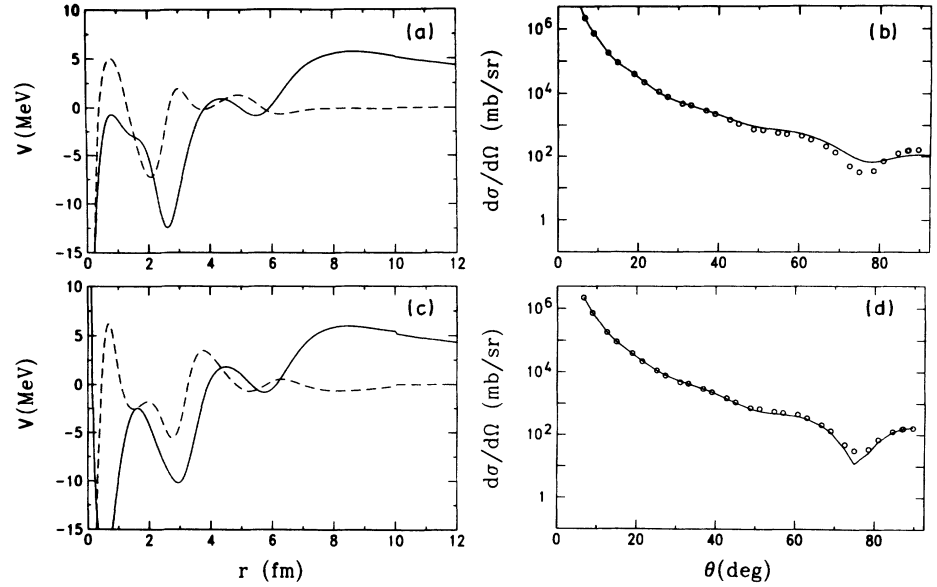

FIG. 2. Results of the conventional inverse scattering calculation with methods C1 and C′1 at $E_{\text{c.m.}}$=7.998 MeV. (a) real (——) and imaginary (- - - -) part of the inverted potentials obtained by method C1; (b) reproduction (——) of the experimental data (o o o) by the inverted potential using method C1 which gives χ^2_V = 609.8; (c) and (d) the same as (a) and (b) but with method C′1 giving χ^2_V = 60.8. Related phase shifts are listed in Table I.

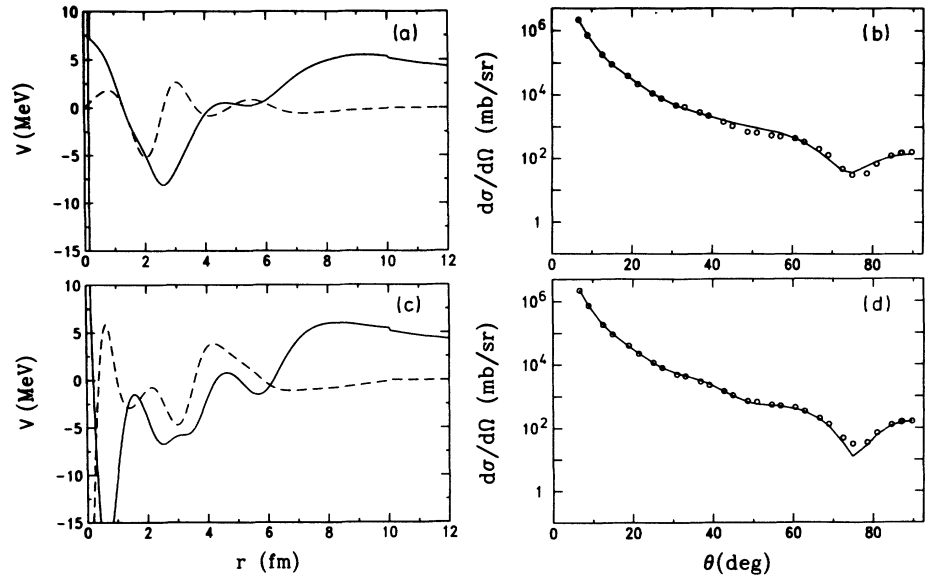

FIG. 3. Results of the unified inverse scattering calculation with methods M1 and M′1 at $E_{\text{c.m.}}$=7.998 MeV. (a): real (——) and imaginary (- - - -) part of the inverted potentials obtained by method M1; (b): reproduction (——) of the experimental data (o o o) by the inverted potential using method M1 which gives χ^2_V = 275.0; (c) and (d): the same as (a) and (b) but with method M′1 giving χ^2_V = 61.9. Related phase shifts are listed in Table II.

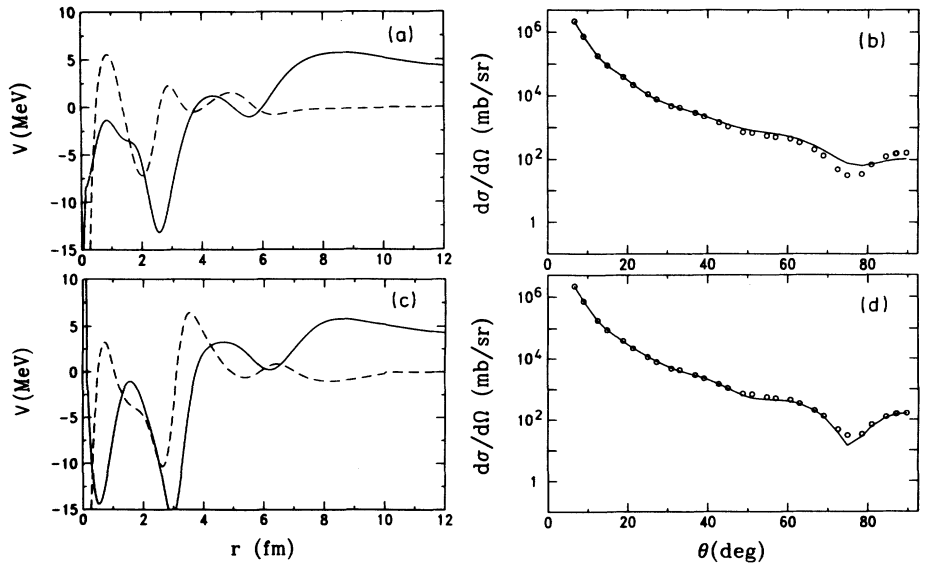

FIG. 4. Results of the unified inverse scattering calculation with methods M2 and M′2 at $E_{\text{c.m.}}$ = 7.998 MeV. (a): real (——) and imaginary (- - - -) part of the inverted potentials obtained by method M2; (b): reproduction (——) of the experimental data (o o o) by the inverted potential using method M2 which gives χ^2_V = 597.1; (c) and (d): the same as (a) and (b) but with method M′2 giving χ^2_V = 71.6. Related phase shifts are listed in Table III.

TABLE II. Real and imaginary parts of the matrix elements S_l obtained by the unified methods M1 and M′1 applied to the $^{12}C+^{12}C$ scattering data [6] at $E_{c.m.} = 7.998$ MeV. The search was based on the error square expressions χ_c^2 and χ'^2_c given by Eqs. (7). The real phase shifts δ_l^R and absorption coefficients η_l are listed also. The potentials and cross sections corresponding to this table are shown in Fig. 3.

l	$\mathrm{Re}S_l$[a]	$\mathrm{Im}S_l$[a]	$\delta_l^{R\,a}$	η_l[a]	$\mathrm{Re}S_l$[b]	$\mathrm{Im}S_l$[b]	$\delta_l^{R\,b}$	η_l[b]
0	−0.5498	−0.8353	8.3483	1.0000	0.3129	−0.3108	9.0337	0.4410
1	0.2262	0.3045	6.7491	0.3793	−0.2394	0.3547	7.3655	0.4279
2	−0.0136	−0.1863	5.4614	0.1868	0.0749	−0.5876	5.5611	0.5924
3	−0.4646	−0.0092	4.7223	0.4647	−0.4740	0.3819	4.3733	0.6087
4	0.6672	0.4959	3.4612	0.8313	0.1875	−0.0927	2.9120	0.2092
5	−0.8385	−0.2553	1.7186	0.8765	−0.3929	0.0742	1.4775	0.3998
6	0.9556	0.1266	0.0659	0.9639	0.6992	−0.2287	−0.1581	0.7357
7	−0.2206	−0.0587	−1.4408	0.2283	−0.8177	−0.0360	−1.5488	0.8185
8	0.8331	0.2858	0.1652	0.8808	0.7684	−0.2756	−0.1722	0.8164
9	0.8699	0.1583	0.0900	0.8842	0.8790	−0.2232	−0.1243	0.9069
10	0.8640	0.0450	0.0260	0.8652	0.9454	−0.1450	−0.0761	0.9565
11	0.8782	−0.0257	−0.0146	0.8786	0.9826	−0.0792	−0.0402	0.9858
12	0.9124	−0.0482	−0.0264	0.9137	0.9994	−0.0374	−0.0187	1.0000

[a]Method M1: minimization of χ_c^2 (with the result $\chi_c^2 = 6.56$; the corresponding inverted potential gives $\chi_V^2 = 275.0$)
[b]Method M′1: minimization of χ'^2_c (with the result $\chi'^2_c = 0.00149$; the corresponding inverted potential gives $\chi_V^2 = 61.9$).

ues of χ_V^2=275.0, 61.9 for the M1, M′1 methods, and of χ_V^2=597.1, 71.6 for the M2, M′2 methods, respectively. In all cases the PS procedure has been applied to the minimization of the expressions χ_c^2 and χ'^2_c with initial spectral coefficients taken from the related conventional calculations. The other parameters of the conventional calculations have been adopted as well.

In Figs. 3 and 4 no dramatic change in the potential shapes can be observed when compared to the results shown in Fig. 2. All the potentials obtained by the six methods C1, C′1, M1, M′1, M2, M′2 exhibit similar structures. The real part of the potential is characterized by two minima, a strong one at $r \approx 2.5$–3.0 fm, and a weaker one at $r \approx 5.5$–6.0 fm. The maximum of the Coulomb barrier resulting from all six methods lies in the region of $r \approx 8.5$ fm, a smaller radius than the matching radius (r_0) fixed at 10 fm. At this matching radius a small mismatch of magnitude produced by the methods M1 and M′1 [see Figs 3(a) and 3(c)] can be seen. Also the imaginary parts of the potentials are similar, tending to zero in the outer regions and exhibiting positive values in the reaction zone suggesting a feed back of the probability flux from the inelastic and reaction channels to the elastic one.

The similarity of the potential shapes can be explained by the fact that the optimization of the spectral coefficients (by the PS procedure) yields no dramatic changes of the corresponding phase shifts δ_l $(0,1,\ldots,l_{\max})$ presented in Tables II and III. This holds true for the values belonging to the $l = 7$ partial wave as well which has

TABLE III. Real and imaginary parts of the matrix elements S_l obtained by the unified methods M2 and M′2 applied to the $^{12}C+^{12}C$ scattering data [6] at $E_{c.m.}$=7.998 MeV. The search was based on the error square expressions χ_c^2 and χ'^2_c given by Eqs. (7). The real phase shifts δ_l^R and absorption coefficients η_l are listed also. The potentials and cross sections corresponding to this table are shown in Fig. 4.

l	$\mathrm{Re}S_l$[a]	$\mathrm{Im}S_l$[a]	$\delta_l^{R\,a}$	η_l[a]	$\mathrm{Re}S_l$[b]	$\mathrm{Im}S_l$[b]	$\delta_l^{R\,b}$	η_l[b]
0	−0.4935	−0.8697	8.3813	1.0000	0.1292	−0.3426	8.8197	0.3662
1	0.1742	0.6267	6.9330	0.6505	−0.1190	0.1282	7.4427	0.1749
2	−0.0244	−0.1614	5.4228	0.1633	0.0844	−0.6122	5.5663	0.6180
3	−0.4547	0.2432	4.4668	0.5156	−0.7885	0.6148	4.3813	0.9999
4	0.6447	0.5169	3.4795	0.8264	0.2386	−0.0906	2.9602	0.2552
5	−0.8483	−0.3640	1.7735	0.9231	−0.4389	0.1500	1.4062	0.4638
6	0.9727	0.1680	0.0855	0.9871	0.6665	−0.2601	−0.1860	0.7154
7	−0.1904	−0.0398	−1.4677	0.1945	−0.7276	−0.1197	−1.4893	0.7373
8	0.8276	0.2917	0.1695	0.8775	0.7997	−0.2403	−0.1460	0.8350
9	0.8513	0.1703	0.0987	0.8682	0.8493	−0.1826	−0.1059	0.8687
10	0.8489	0.0572	0.0336	0.8508	0.9105	−0.1329	−0.0725	0.9201
11	0.8867	0.0089	0.0050	0.8868	0.8448	−0.1637	−0.0957	0.8605
12	0.9177	−0.0364	−0.0198	0.9184	0.9996	−0.0293	−0.0147	1.0000

[a]Method M2: minimization of χ_c^2 (with the result $\chi_c^2 = 6.33$; the corresponding inverted potential gives $\chi_V^2 = 597.1$).
[b]Method M′2: minimization of χ'^2_c (with the result $\chi'^2_c = 0.00224$; the corresponding inverted potential gives $\chi_V^2 = 71.6$).

been crucial in obtaining a smooth potential shape. The arbitrary value of $\delta_7^R=-1.5$ that was set by "hand" has changed to -1.44 and -1.55 in the M1 and M′1 methods, and to -1.47 and -1.49 in the M2 and M′2 ones, respectively. The changes in the absorption coefficients seem to affect the shape of the real potential only rather weakly.

The task of selecting an optimal procedure out of six methods C1,. . ., M′2 investigated cannot be solved unambiguously. As shown by Figs. 2–4, all the six methods give qualitatively the same results. Therefore, we follow the principle of favoring that method which (i) results in the smallest value of χ_V^2, and (ii) provides a smooth potential shape. The first criterium is connected with the consistency of the inverse calculation; the second one is introduced since heavy ion potentials obtained so far within different frameworks behave smoothly. Although the inverse scattering calculation is unique, we note that smaller values of χ_V^2 can be obtained in some cases. But then the potentials are very oscillatory and violate our criterium (ii).

B. The inverted potentials obtained by the unified methods for the scattering system $^{12}C+^{12}C$ in the energy range of $E_{c.m.} \approx 8$–12 MeV

Figure 5 shows the potentials obtained by inversion of the elastic $^{12}C+^{12}C$ data for scattering energies $E_{c.m.}$ ≈8–12 MeV. The real part of the inverted potentials, $\mathrm{Re}V(R)$, is shown on the left side and the imaginary part, $\mathrm{Im}V(r)$, on the right side of Fig. 5. Specifically the calculations have been carried out at eight scattering energies: viz. 7.988, 8.535, 9.057, 9.48, 10.533, 10.954, 11.503, and 12.077 MeV. These energies, rounded off to one significant decimal digit, are also indicated in the middle part of Fig. 5. The potentials shown in Fig. 5 are arranged vertically from top to bottom according to increasing energy. With increasing energy these potentials were obtained by the methods (indicated also in Table IV) C′1, C1, M′1, C1, M2, M2, M1, C′1, respectively, for which the following values of χ_V^2, rounded off to integer numbers, are 61, 101, 22, 16, 74, 53, 110, and 216. Note that the results at $E_{c.m.}$=9.480 and 11.503 MeV compare very well with those presented in Ref. [5] at $E_{c.m.}$ = 9.50 and 11.38 MeV. The technical parameters used are listed in Table IV.

In general, the inversion potentials differ in shape from Woods-Saxon form. The real parts of the potentials vary in value between -10 and 9 MeV, taking a maximum value at distances $r \approx 8$–8.5 fm. As a rule, the imaginary parts of the potentials are smaller in magnitude than the real ones. The formation of a Coulomb barrier of height 6.2 MeV at distances $r \approx 8.4$–8.8 fm seems to support the initial assumption that the scattering is governed by a pure Coulomb potential beyond a matching radius (chosen to be 10 fm). In two or three cases a very small mismatch between the outer Coulomb potential and the inner inverted (complex) potentials can be observed. These minor discontinuities may arise from the neglect of higher partial waves and/or from the numerical approximations that are always a feature of numerical calculations.

The imaginary (absorptive) parts of the potentials have the same range as the real ones. In all cases they have a shallow absorbing (negative) part in the outer region. They contain several positive maxima as well which are located mainly at radii where the real parts have minimum values. Positive imaginary parts of the potentials mean a back-feeding of the probability current from the inelastic channels into the elastic one, and they are similar to those investigated by Wolf and Mosel [14] for the same scattering system and using the Feshbach formalism.

An interesting shape transition of the potentials occurs as a function of the incident energy between $E_{c.m.}$ = 9 and 10.5 MeV. This is shown in Fig. 5. Considering the real part of the potentials, the main feature of this shape transition is a gradual disappearance of the smaller outer minimum at $r \approx 6.0$ fm and a reappearance of the strong internal minimum at radial distances $r \approx 2.4$–3

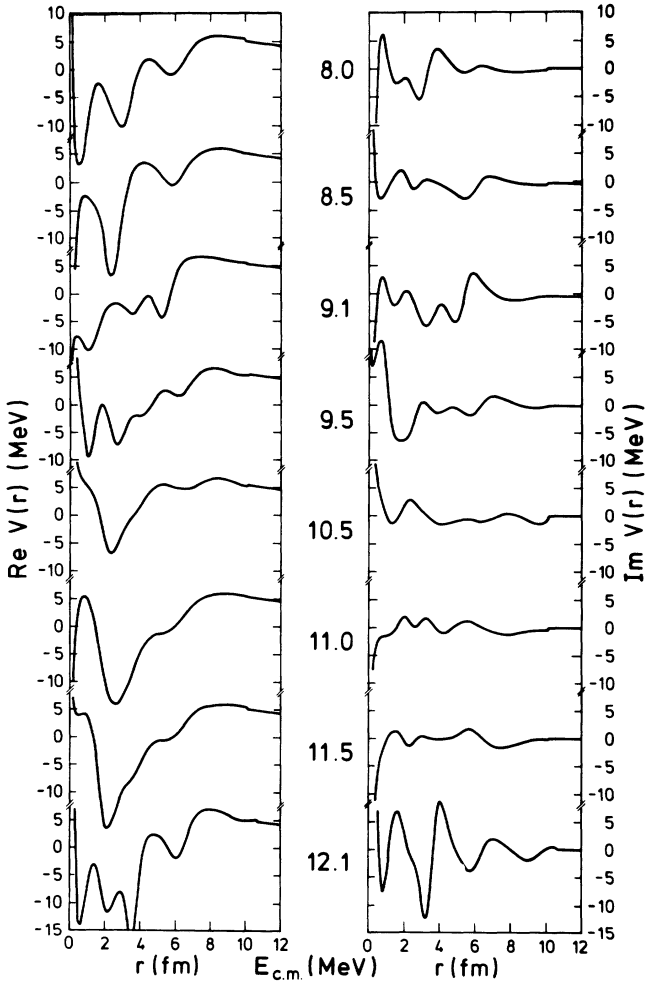

FIG. 5. Real part and imaginary part of the inverted potentials obtained by various inverse methods as described in the text for the eight energies indicated in the middle part of the figure. Elastic angular distributions calculated with these potentials are shown by the solid lines in Fig. 1.

fm. The inner minimum reappearing at $E_{\text{c.m.}} = 10.5$ MeV remains the dominant structure of the real part of the potential at higher energies. According to the calculation of May and Scheid [15], the inverted potential at the scattering energy of $E_{\text{c.m.}} = 18.5$ MeV is characterized by only one strong minimum at $r \approx 4.2$ fm. In this connection it would be interesting to study how the real part of the potential evolves from the shape at $E_{\text{c.m.}} = 12.1$ MeV (depicted on the bottom of Fig. 5) into that given in Ref. [15] for $E_{\text{c.m.}} = 18.5$ MeV. One can infer from Fig. 5 that the change might not be large since the two forms of the real parts of the potentials at $E_{\text{c.m.}} = 12.1$ MeV and $E_{\text{c.m.}} = 18.5$ MeV given in Ref. [15] are similar. The main difference is the different position of the characteristic minimum.

At smaller and higher scattering energies ($E_{\text{c.m.}} = 8.0$, 8.5, 9.1, 12.1 MeV), the real part of the potential also exhibits a secondary minimum at $r \approx 5.5$–6.2 fm. This minimum could be the reason why a double minimum Woods-Saxon potential introduced by Ordonez *et al.* [16] has been so successful in fitting the $^{12}C+^{12}C$ scattering data at higher energies.

For very small relative distances, one observes a singularity in the potentials. That is of mathematical origin in the Newton-Sabatier method and well known to arise because of the $1/\tilde{\rho}$ dependence of Eq. (16) for a finite number of angular momenta. Fortunately, the inner part of the potential does not contribute too much in evaluations of the cross section as proved by numerical calculations [15].

The inverted complex potentials shown in Fig. 5 can be used to calculate phase shifts and cross sections over a broader energy band around the incident energy to which the potential itself belongs. With such calculations we obtained an insight into the resonance structures of the colliding nuclear system $^{12}C+^{12}C$. We studied the resonances of the elastic cross sections and identified the partial waves responsible for them. In Table IV those resonant partial waves l_{res} which provide phase shifts $\delta^R_{l_{\text{res}}}(E \approx E_{\text{c.m.}})=\pi/2$ in the corresponding inverted potential belonging to $E_{\text{c.m.}}$ are identified. If one compares these resonating partial waves with those given in Ref. [13] close agreement is found. Also, the appearance of the value $l_{\text{res}} = 5$ for $E_{\text{c.m.}} = 8$ MeV should be noted. That coincides with the phase δ^R_5 that had to be fixed in the conventional inverse calculation discussed in Sec. III A.

IV. SUMMARY AND COMMENTS

The conventional inverse quantum scattering calculation starts with phase shifts obtained by a phase shift analysis of experimental cross sections and then uses an inversion scheme for which the phase shifts are input data. The unified method investigated in this paper joins the two separate steps of the conventional method. The analysis of the experimental data is performed with respect to the spectral coefficients $\{c_l\}$ $(l = 0, 1, \ldots, l_{\max})$ of the modified Newton-Sabatier inversion method. In case of elastic scattering of identical particles with zero spin, the unified method yields also the phase shifts of odd partial waves which do not contribute to the cross section. The input quantities are measured differential cross sections with experimental errors, output results are complex, energy dependent potentials. In practice we recommend that the method starts with an initial set of spectral coefficients obtained via a conventional calculation. Then application of the unified method gives an improved inversion potential.

At present, a disadvantage of our program for the modified Newton-Sabatier method is the large square errors, χ^2_V, listed in Table IV. These large errors arise mainly from very small differential cross sections between 70° and 90°, and can have different origins, such as the choice of the upper angular momentum $l_{\max}$, of the matching radius r_0, and of the radii $\tilde{r}_1$, $\tilde{r}_2$, $\tilde{r}_3$. But we have tested that the chosen $l_{\max}$ is sufficient in the considered cases. Also the selected radii have a negligible effect on the accuracy of the results. However, this program has to solve linear equations that are nearly singular.

The elastic potentials we have obtained for the $^{12}C+^{12}C$ system and their systematic energy dependence in a small interval of energy are novel. At nearly all energies a shallow minimum in the real potential has been observed at internuclear distances of 5–6 fm. Possibly that is caused by quasimolecular ^{12}C cluster configurations. The prominent minimum at 2–3 fm can be interpreted as originating from the configurations of the

TABLE IV. The values of the parameters used in the inverse calculations of the potentials presented in Fig. 5. The second column identifies the method that was applied. Error squares χ^2_V characterizing the quality of the inverted potential V are listed in the third column. The fourth column lists the angular momentum l_{res} of the resonating partial waves where the real phase shifts pass through $\pi/2$ in the vicinity of $E_{\text{c.m.}}$. The fifth column gives the angular momentum $l^{\text{ReV}}_{\text{res}}$ of the resonating partial waves in the real potential. The remaining columns give information about the technical parameters $l_{\max}$, r_0, and $\tilde{\rho}_i$ used in the calculations.

$E_{\text{c.m.}}$ (MeV)	Method	χ^2_V	l_{res}	$l^{\text{ReV}}_{\text{res}}$	$l_{\max}$	r_0 (fm)	$\tilde{\rho}_1$	$\tilde{\rho}_2$	$\tilde{\rho}_3$	$\tilde{\rho}_4$
7.988	C′1	61	5,7	7	12	10.0	11.5	12.5	13.5	
8.535	C1	101	5,7	5,7	12	10.0	12.5	13.5	14.5	
9.057	M′1	22	7	7	12	10.0	12.75	13.75	14.75	
9.48	C1	16	7	7	14	10.0	13.0	14.0	15.0	16.0
10.533	M2	74	6	6	12	10.0	13.5	14.5	15.5	
10.954	M2	53	7,9	7,9	14	10.0	15.5	16.5	17.5	
11.503	M1	110	7	7	14	10.0	15.5	16.5	17.5	
12.077	C′1	216	7	-	14	10.5	16.0	17.0	18.0	

prolately deformed ^{24}Mg nucleus. The situation with respect to two potential minima found in this study is very similar to the one already discussed by Ordonez *et al.* [16] at higher energies, but it is different to the case at $E_{c.m.}=18.5$ MeV where only one minimum at $r = 4.2$ fm has been seen [15].

The real and imaginary parts of the potential relate to each other. The structures of the imaginary part are correlated with those of the real potential. At radii where the real potential has its second (quasimolecular) minimum, the imaginary potential is positive with the consequence that it supports the existence of molecular states of two touching ^{12}C nuclei. Positive imaginary parts mean a backfeeding from inelastic channels to the elastic one and absorptive potentials of that kind have never been taken into account in potential fits of heavy ion differential cross sections. Indeed, we believe that such absorptive potentials must be considered in future studies of heavy ion collisions.

This work was supported by GSI (Darmstadt), DFG/MTA-45, and OTKA (517, 518, T 7283).

[1] R. G. Newton, J. Math. Phys. **3**, 75 (1962); P. C. Sabatier, J. Math. Phys. **7**, 1515 (1966); **7**, 2079 (1966); R. G. Newton, *Scattering of Waves and Particles* (Springer, New York, 1982); K. Chadan and P. C. Sabatier, *Inverse Problems in Quantum Scattering Theory* (Springer, Berlin, 1977).

[2] C. Marty, in *Resonances in Heavy Ion Reactions*, Vol. 156 of *Lecture Notes in Physics*, edited by K. A. Eberhard (Springer, Berlin, 1982), p. 216; H. D. Helb and H. Voit, Nucl. Phys. **A204**, 196 (1973); W. Tiereth, Z. Basrak, N. Bischof, H. Fröhlich, and H. Voit, *ibid.* **A440**, 143 (1985); W. Treu, H. Fröhlich, W. Galster, P. Dück, and H. Voit, Phys. Rev. C **18**, 2148 (1978); W. Treu, Dissertation, Erlangen, 1980 (unpublished).

[3] M. Münchow and W. Scheid, Phys. Rev. Lett. **44**, 1299 (1980).

[4] K.-E. May, M. Münchow, and W. Scheid, Phys. Lett. **141B**, 1 (1984).

[5] B. Apagyi, A. Ostrowski, W. Scheid, and H. Voit, J. Phys. G **18**, 195 (1992).

[6] W. Treu, H. Fröhlich, W. Galster, P. Dück, and H. Voit, Phys. Rev. C **22**, 2462 (1980); W. Treu, H. Fröhlich, P. Dück, and H. Voit, *ibid.* **28**, 237 (1983).

[7] L. J. Schiff, *Quantum Mechanics* (McGraw-Hill, New York, 1968).

[8] A. Schmidt, Diploma thesis, University Giessen (1992), unpublished.

[9] W. L. Price, The Computer Journal **20**, 367 (1977).

[10] R. Hooke and T. A. Jeeves, J. Assoc. Computing Machinery **8**, 212 (1961).

[11] M. Abramowitz and I. A. Stegun, *Handbook of Mathematical Functions* (Dover, New York, 1972).

[12] K.-E. May, Ph.D. thesis, University Giessen (1988), unpublished.

[13] H. Voit, W. Galster, W. Treu, H. Fröhlich, and P. Dück, Phys. Lett. **67B**, 399 (1977); D. R. James and N. R. Fletcher, Phys. Rev. C **17**, 2248 (1978); U. Abbondanno, *A Collection of Data on Resonances in Heavy-Ion Reactions* (INFN/BE-91/11, 1991, unpublished).

[14] R. Wolf and U. Mosel, Z. Phys. A **305**, 179 (1982).

[15] K.-E. May and W. Scheid, Nucl. Phys. **A466**, 157 (1987).

[16] C. E. Ordonez, R. J. Ledoux, and E. R. Cosman, Phys. Lett. B **173**, 39 (1986).